Surface Topographies of Glaucoma Drainage Devices and Their Influence on Human Tenon Fibroblast Adhesion

Lars Choritz,[1] *Kaloian Koynov,*[2] *Giulia Renieri,*[1] *Keith Barton,*[3] *Norbert Pfeiffer,*[1] *and Hagen Thieme*[1]

Purpose. This study was performed to investigate the surface topography of different glaucoma drainage devices and to determine the effects of surface roughness on cell adhesion of cultured human tenon fibroblasts.

Methods. The surface topography of four widely used devices (Ahmed FP7 and Ahmed S-2; New World Medical, Inc., Rancho Cucamonga, CA; Baerveldt BG101-350; Advanced Medical Optics, Irvine, CA; and Molteno S1; Molteno Ophthalmic Ltd., Dunedin, New Zealand) was investigated by scanning electron microscopy, and roughness was quantified by white-light confocal microscopy. Cells were grown for 72 hours on the surfaces of implants affixed to standard culture dishes. The cells were labeled with a fluorescent dye and detected by confocal laser scanning microscopy, while simultaneously imaging the surface reflectance. Collagen adsorption was quantified immunologically by using fluorescent beads coupled to a secondary antibody.

Results. The root-mean-square roughness was 1.5 ± 0.1 μm (mean ± SE) for the silicone Ahmed model FP7 and 1.3 ± 0.1 μm for the Ahmed with polypropylene base plate Ahmed model S-2. The Baerveldt was substantially smoother, with a mean roughness of 0.1 ± 0.01 μm. The Molteno was the smoothest of all devices (0.07 ± 0.01 μm). Cell adhesion was most prevalent on base plates with higher surface roughness, markedly less pronounced on the smoother base plates, and independent of collagen adsorption.

Conclusions. The most frequently implanted glaucoma drainage devices are of markedly different surface topography. Surface roughness appears to correlate with tenon fibroblast adhesion in vitro and also with the rate of occurrence of postimplantation hypertensive phase and failure due to fibrous encapsulation. Surface roughness may thus play a role in triggering excessive fibrovascular reactions. Smoother base plate surfaces may enhance the success rates of these devices. (*Invest Ophthalmol Vis Sci.* 2010;51:4047–4053) DOI:10.1167/iovs.09-4759

From the [1]BiomaTiCS Research Group, Department of Ophthalmology, University Medical Center, Johannes Gutenberg University, Mainz, Germany; the [2]Max-Planck-Institute for Polymer Research, Mainz, Germany; and the [3]Moorfields Eye Hospital, London, United Kingdom.

Supported in part by the BiomaTiCS Research Group of the University Medical Center of the Johannes Gutenberg University.

Submitted for publication October 11, 2009; revised February 7 and 19, 2010; accepted February 22, 2010.

Disclosure: **L. Choritz**, None; **K. Koynov**, None; **G. Renieri**, None; **K. Barton**, None; **N. Pfeiffer**, None; **H. Thieme**, None

Corresponding author: Hagen Thieme, Department of Ophthalmology, University Medical Center, Johannes Gutenberg University, Langenbeckstrasse 1, 55131 Mainz, Germany; thieme@augen.klinik.uni-mainz.de

Glaucoma drainage devices (GDDs) have become widely accepted in the surgical treatment of glaucoma. Although most surgeons favor their use in complicated cases, in which conventional surgical procedures such as trabeculectomy have failed, there has been some recent interest in their use as a primary surgical intervention for glaucoma.[1,2] Often the long-term success of these devices is limited by failure to control IOP because of fibrous encapsulation of the implant base plate, similar to the encapsulation that is seen after other filtering procedures.[3,4] In contrast to their effect in trabeculectomy, antiproliferative substances like mitomycin C or 5-fluoruracil fail to improve the long-term success of GDDs.[5,6] Encapsulation, especially in pediatric patients, can lead to early failure of the implant, sometimes requiring surgical removal of the capsule or even explantation of the device.[7,8]

The stimuli for bleb fibrosis are not fully understood. In addition to patient-related factors such as aqueous humor TGF-β_2,[9] TGF-β receptor expression in tenon fibroblasts[10] and previous failed ocular surgical procedures,[11] several implant-related factors are probably important. Among these, the choice of biomaterial is believed to influence the initial inflammatory response to the implant,[12] whereas shape, size, and rigidity of the base plate are thought to influence fibroblast growth and extracellular matrix (ECM) deposition through mechanically induced activation of the cells.[13–15]

One aspect of implant design that has been largely ignored is the surface texture of the base plate. Since the surface constitutes the major site of interaction with the surrounding tissue, topographic features as well as surface chemistry may well influence wound healing and the fibrotic response. This study was performed to investigate the surface texture of four commonly used GDDs and their effect on cell adhesion and growth of human tenon fibroblasts.

Methods

Drainage Devices

Four different GDDs from three different manufacturers were used in the study. These included the Ahmed Glaucoma Valve (AGV) models FP7 (with a silicone base plate) and S-2 (the older model with a polypropylene base plate; New World Medical, Inc., Rancho Cucamonga, CA), the Baerveldt Glaucoma Implant (BGI) model BG101-350 (silicone; Advanced Medical Optics, Irvine, CA), and the Molteno Drainage Implant (MDI) single-plate model S1 (polypropylene; Molteno Ophthalmic, Ltd., Dunedin, New Zealand; Fig. 1). All devices were purchased from regular distributors and kept sterile until use.

Human Tenon Fibroblast Cell Culture

Small samples of approximately 1 to 2 mm^3 of Tenon's capsule were obtained during routine cataract or glaucoma surgery from donors who had given prior written consent. The samples were transferred to a

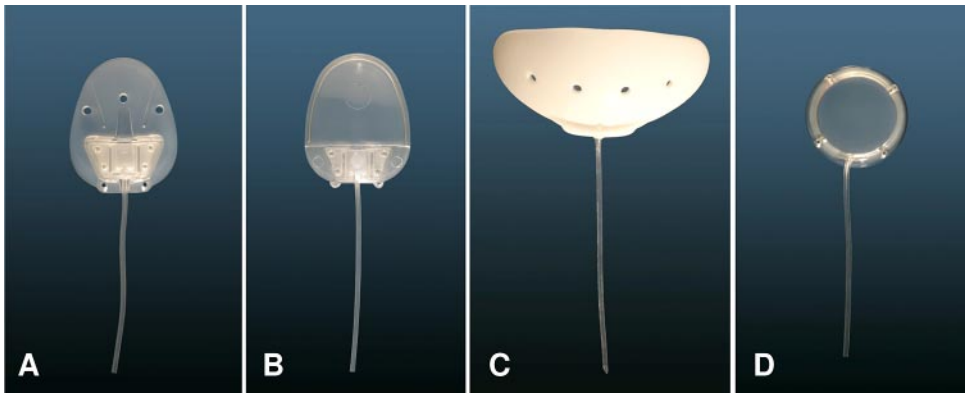

FIGURE 1. Devices investigated. (**A**) AGV FP7 (silicone base plate), (**B**) AGV S-2 (polypropylene base plate), (**C**) BGI BG101-350 (silicone), and (**D**) MDI S1 (polypropylene). All devices were photographed at the same scale.

standard 60-mm cell culture dish, covered with a 20-mm glass coverslip, supplied with culture medium (Dulbecco's modified Eagle's medium [DMEM] supplemented with 10% fetal calf serum [FCS] and 1% penicillin/streptomycin), and placed in a 37°C, 5% CO_2-containing incubator. After 1 to 2 weeks, when the cells had grown out approximately 1.5 cm from the tissue sample, they were passaged into 25-cm^2 culture flasks by using the trypsin/EDTA method. This passage was considered the first. All further passages were treated with the same method, with the cells being divided into three equal fractions each time. Seven individual cell lines were established in this fashion, dubbed HTF-1 to -7, three of which (HTF-1, -3, and -7, randomly chosen) were used for the cell experiments in this study. Cell identity was confirmed by immunocytochemical staining for Thy-1 with the monoclonal antibody AS02 (Dianova, Hamburg, Germany; data not shown). Cells from the fourth passage were used in the study. Tissue procurement and all experiments adhered strictly to the Declaration of Helsinki.

Scanning Electron Microscopy

Surface images of base plates (both top and bottom sides); silicone tubes; and, where applicable, the valve mechanism, were obtained by scanning electron microscopy (SEM; Gemini 1530 microscope; Carl Zeiss Meditec AG, Oberkochen, Germany; or a Nova 600 Nanolab Dualbeam system; FEI Company, Eindhoven, The Netherlands).

Profilometry by White-Light Confocal Microscopy

Representative surface areas from the base plates of all devices were scanned by 3-D white-light confocal microscopy (μSurf; NanoFocus AG, Oberhausen, Germany). Using the system software, we measured the surface profile along a randomly chosen line through each scanned section. For topographic comparison, we used the root mean square (RMS) as a basic standard parameter of surface roughness (Fig. 2).

Cell Attachment on Implant Surfaces Determined by Confocal Laser Scanning Microscopy (CLSM)

To compare the ability of human tenon fibroblasts to adhere to the native implant surfaces of the four chosen devices, we affixed the base plate of each device to a standard cell culture dish with a small amount of a clear two-component silicone (Elastosil RT 604; Wacker Chemie, Burghausen, Germany). An equal number of fourth-passage tenon fibroblasts from primary human cultures ($\sim 10^4$ cells per dish) were seeded onto the base plates and allowed to grow for 72 hours in DMEM, supplemented with 10% FCS, 1% penicillin/streptomycin at 37°C in a 5% CO_2-containing incubator. After 72 hours, the medium was discarded, and the cells were gently rinsed with PBS and stained (Cell Tracker Green CMFDA; Molecular Probes, Invitrogen, Carlsbad, CA) for 30 minutes, according to the manufacturer's instructions. Excess dye was washed off with PBS, the culture medium was replaced and the culture dishes were reincubated for 8 hours.

Images of the cells on the upper surface of each base plate were obtained (SP2 confocal laser scanning microscope; Leica, Wetzlar, Germany). With simultaneous measurements of the fluorescence of the cell tracker dye (excitation wavelength, 488 nm by argon-ion laser) and the reflectance of a helium-neon laser (632.8 nm) from the surface, it was possible to image the cells and the surface at the same time (Fig. 3). Because of the macroscopic curvature of the base plates used in this study, it was necessary to combine series of images from up to 50 focal planes at the same position to display a complete 1.5 mm × 1.5 mm square of each surface.

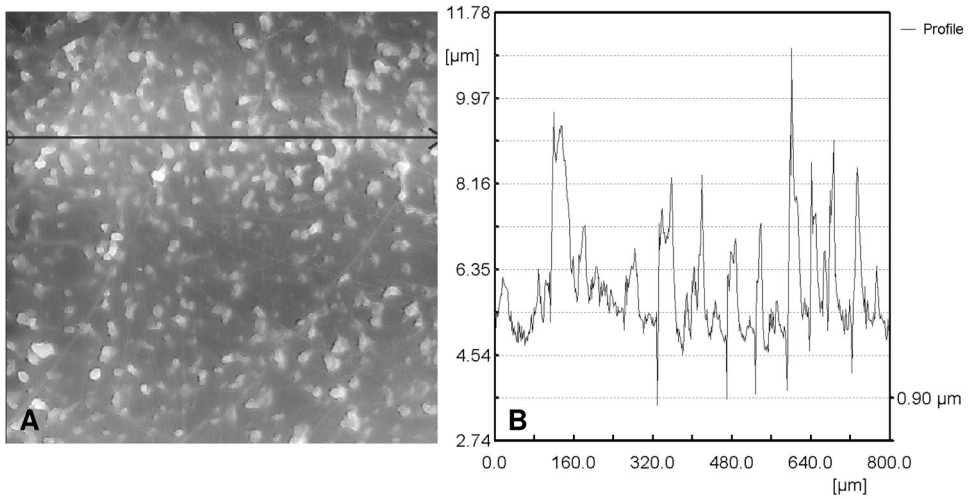

FIGURE 2. Typical profilometric measurement. *Arrow* in the white-light CLSM image (**A**) indicates the site and direction of measurement of the profile shown in (**B**). Area, 800 μm × 800 μm. The RMS was calculated for each measured profile.

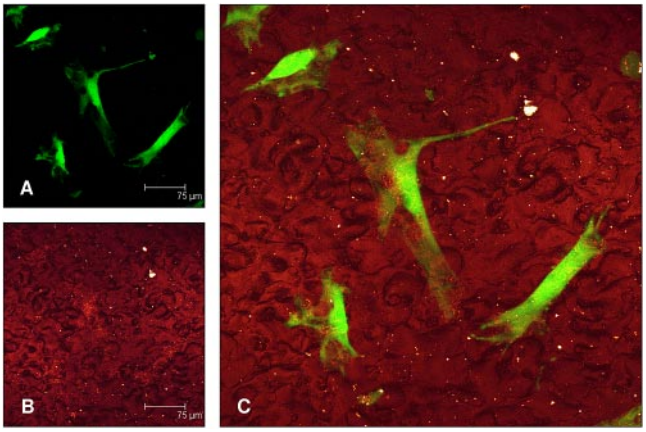

FIGURE 3. Sample image of cells on a surface (AGV FP7) as obtained by CLSM. (**A**) Tenon fibroblasts stained with CMFDA dye, excited at 488 nm. (**B**) Laser light simultaneously reflected from the surface of the implant on which the cells were seeded. A composite image of (**A**) and (**B**) depicts the cells in situ (**C**).

Protein Adsorption on Implant Surfaces

To rule out the confounding effects of surface chemistry on the observed cell adhesion, we quantified adsorption of collagen on the implant surfaces indirectly by an immunologic approach: The devices, fixed in standard culture dishes, as explained earlier, were incubated with a solution containing 1 mg/mL type I collagen from rat tail (PAN Biotech GmbH, Aidenbach, Germany) on a rocking platform at room temperature overnight. After repeated rinsing with PBS+0.1% Tween (PBST), the devices were incubated with 1:2000 polyclonal antibody against type I rat collagen (mouse-anti-rat COL1A, sc-59772; Santa Cruz Biotechnology, Heidelberg, Germany) for 2 hours at room temperature. Excess antibody was washed off with PBST and FITC-labeled secondary antibody (goat-anti-mouse; Meridian Life Science Inc., Saco, ME) coupled to protein-G beads (Dynabeads; Invitrogen Dynal, Oslo, Norway) were added at a concentration of 2×10^6 beads per culture dish. After 1 hour of incubation at room temperature, unbound beads were rinsed off by repeated washing with PBST. The number of beads bound to collagen adsorbed to the implant surface was assessed with the same CLSM set-up described earlier. Because of the small size of the beads (2.8 ± 0.2 μm), a higher magnification was used than that used for the cell counts. Thus, we determined the average number of beads per 375 μm $\times$ 375 μm of surface area.

Statistical Analysis

All measurements were taken at least in triplicate, and representative images were chosen for this report. GDD surface topography was described qualitatively. Cell adhesion was measured as the mean number of cells per 1.5 mm $\times$ 1.5 mm of surface area ($\pm$ SD), protein adsorption was indirectly quantified as the mean number of antibody-coated beads per 375 μm $\times$ 375 μm of surface area ($\pm$SD). Quantitative measurements of the surface roughness are expressed as the RMS ($\pm$SD) of the surface profiles obtained by white-light CLSM.

RESULTS

Topographic Images

Images obtained by white-light CLSM showed very distinct topographic features of the upper base plate surfaces (Fig. 2). The surface texture of the Ahmed devices appeared to be much rougher due to prominent hill-and-valley structures. In contrast, at the same magnification, both the Baerveldt and Molteno implants showed rather smooth surfaces with only a few irregularities. Some comparatively shallow arced ridges and grooves were visible on the surface of the Molteno base plate (Figs. 4D, 5D). SEM images at the same scale showed

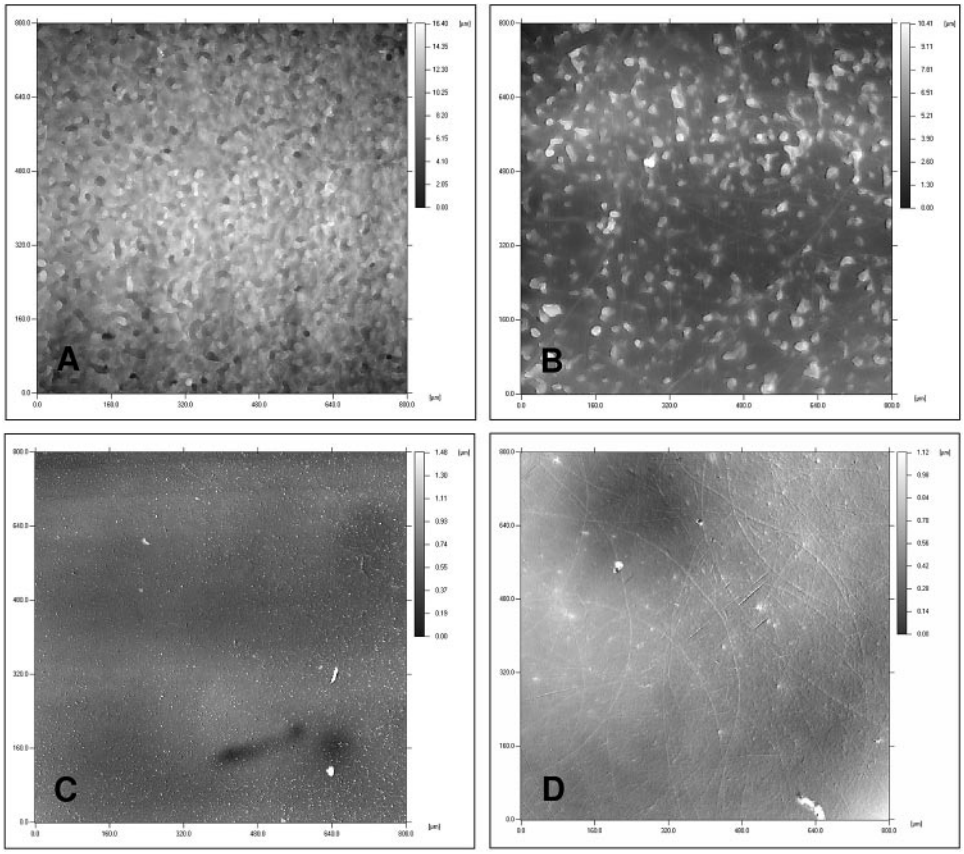

FIGURE 4. Image of surface topography of the base plates of the investigated devices. (**A**) AGV FP7, (**B**) AGV S-2, (**C**) BGI BG101-350, (**D**) MDI S1. Imaging method, white-light CLSM; area, 800 μm $\times$ 800 μm.

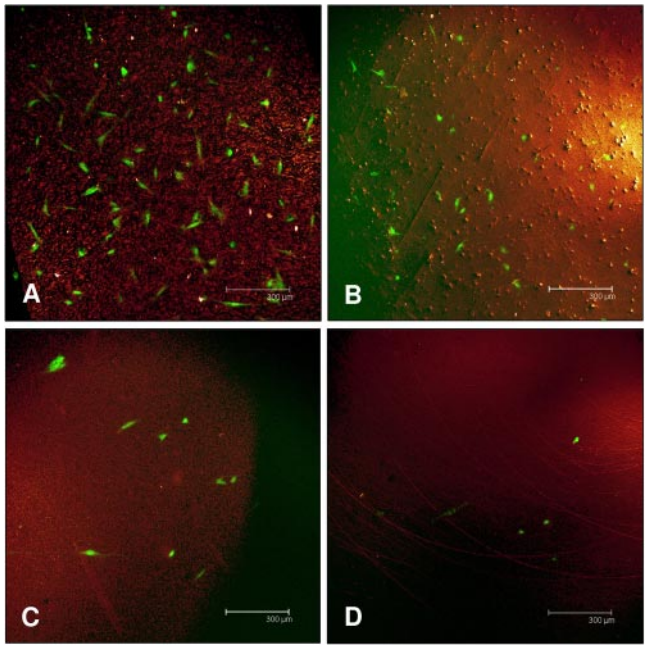

FIGURE 5. Representative images of cells on device surfaces. (**A**) AGV FP7, (**B**) AGV S-2, (**C**) BGI BG101-350, and (**D**) MDI S1.

similar surface features (data not shown). At higher magnification, a different order of roughness was seen with SEM, superposed on the larger hill-and-valley structures of the AGVs. The BGI showed some irregularities at this scale, whereas the MDI base plates were homogenous and smooth (Fig. 6).

Profilometry

Profilometric measurements of the surface roughness confirmed that the silicone AGV (FP7) showed the greatest roughness with an RMS roughness of 1.5 ± 0.1 μm. Similarly, at 1.3 ± 0.1 μm, the polypropylene base plate (S-2) was rather rough. The BGI was substantially smoother at 0.10 ± 0.01 μm for the base plate. The MDI showed an even lower surface roughness than the BGI and overall was the smoothest of all devices (0.07 ± 0.01 μm).

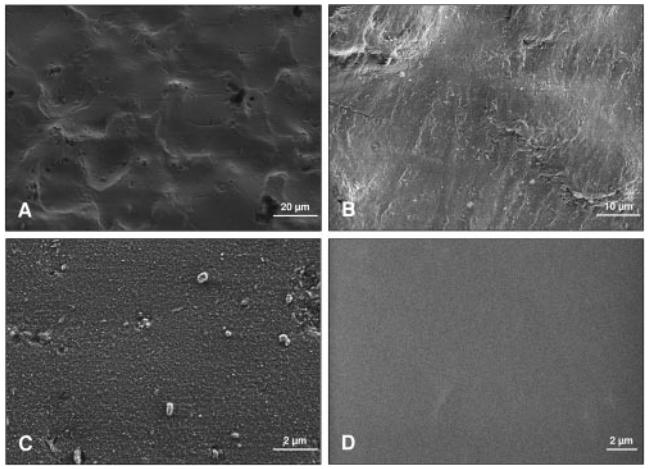

FIGURE 6. High-magnification image of surface details of the devices by SEM. (**A**) AGV FP7, (**B**) AGV S-2, (**C**) BGI BG101-350, and (**D**) MDI S1.

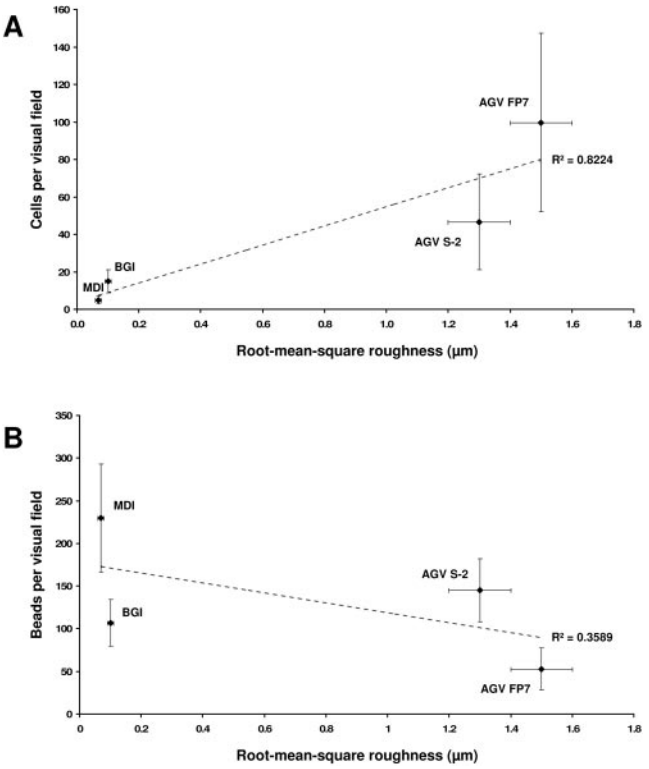

FIGURE 7. (**A**) Number of cells per investigated surface area (1.5 mm × 1.5 mm) plotted against surface roughness as measured by white-light CLSM. There appears to be a correlation between cell count and roughness. (**B**) Number of antibody-coated beads adhering to collagen adsorbed to representative surface areas (375 μm × 375 μm) plotted against surface roughness. There is no apparent correlation between the two parameters.

Tenon Fibroblast Adhesion

Cell adhesion corresponded very well to surface roughness and was most profound on the base plates of the AGVs at 100 ± 24 cells per 1.5 mm × 1.5 mm area for the FP7 model and 47 ± 13 cells for the S-2 model, respectively (n = 4). Fibroblast attachment was considerably less pronounced on the smoother base plates of the BGI (15 ± 3 cells, n = 4) and MDI (5 ± 1 cells, n = 3). The number of cells corresponded well with the measured roughness (R^2 = 0.82; Fig. 7A).

Collagen Adsorption

Collagen adsorption did not correlate with surface roughness or cell adhesion. The mean number of beads bound per 375 μm × 375 μm surface area were 53 ± 24 for the AGV FP7, 145 ± 37 for the S-2 model, 107 ± 27 for the BGI, and 230 ± 63 for the MDI (n = 3 for all devices, R^2 = 0.36, Fig. 7B). Although there was a marked difference between the base plate materials in the number of beads captured by bound collagen (75 ± 19 for silicone vs. 177 ± 38 for polypropylene), an influence of the amount of collagen on cell adhesion was not detected.

DISCUSSION

Since the development of the MDI, which introduced the basic concept of connecting the anterior (or posterior) chamber to a base plate via a silicone tube, many different glaucoma drainage implants have been developed. They drain aqueous into an equatorial subconjunctival bleb, inside which a base plate is

intended to ensure that the bleb area is sufficiently large for adequate aqueous resorption. The BGI is similar in basic design to the MDI, but differs in material (the BGI is made of silicone, whereas the base plate of the MDI is made of polypropylene), size, and shape. The AGV features a flow restrictor intended to prevent hypotony and was first introduced with a base plate manufactured from polypropylene (S-2-type). When it was recognized that the rigidity of this material may have been partly responsible for a higher incidence of encapsulation,[13] the base plate was later replaced by a more flexible model made from silicone, which led to the increased overall success reported in the literature.[16,17]

Even though these implants have been shown to be successful and safe, with short and intermediate term success and complication rates approximately equal to trabeculectomy,[1,18,19] studies of long-term implant survival show a high frequency of failure of IOP control (for review of surgical outcomes, see Schwartz et al.[20]). Moreover, this failure rate does not seem to be significantly reduced by the use of antifibrotic drugs such as mitomycin C.[5,6,21]

It is generally accepted that final IOP largely depends on the amount of aqueous humor resorbed from the bleb that forms because of aqueous drainage around the base plate. The size of the base plate is directly responsible for the size of the aqueous resorption area and thus correlates inversely with IOP, up to an upper size limit of 350 mm^2, above which there appears to be no further decrease of IOP.[22–24] Histopathologic studies show that resorption is restricted by the formation of a fibrous capsule around the base plate during the course of normal wound healing and that the thickness of the proliferative fibrovascular layer of this capsule directly correlates with final IOP.[3]

The incidence of implant failure due to excessive fibrotic encapsulation varies considerably from study to study and between the different devices. In many reports, bleb encapsulation or fibrosis were not explicitly mentioned. Since the capsular thickness correlates with IOP, however, the occurrence of a hypertensive phase within approximately 1 month of GDD implantation as well as the increasing need for adjunctive medication over time in some GDD models is likely to be an indication of excessive fibroblast proliferation and ECM deposition.

It is interesting to note that there were marked differences between the incidences of hypertensive phases in the different implant models. While reports of a hypertensive phase in patients receiving an MDI or BGI are only anecdotal (estimated 20%–30%),[4,20] high IOP develops within weeks after implantation in up to 83.5% of the patients provided with an AGV[25,26] (Table 1).

TABLE 1. Studies Reporting on Hypertensive Phases after GDD Implantation

Study	Device	Patients (*n*)	Hypertensive Phase (%)
Stewart et al.[27]	Molteno SP	38	31.6
Lloyd et al.[28]	Baerveldt	18*	38.9
Ayyala et al.[26]	Molteno DP	30	43.5
	Ahmed	30	83.5
Ayyala et al.[25]	Ahmed	85	82.4
Susanna[29]	Ahmed	92	46.8
Nouri-Mahdavi and Caprioli[30]	Ahmed	156	56.4
Wu et al.[31]	Ahmed	19	63.2
Hong et al.[4]	Baerveldt/Molteno		20–30†
Schwartz et al.[20]	Baerveldt/Molteno		20–30†

SP, single plate; DP, double plate.

* Rabbit model.

† Estimates based on indirect evidence from reports without explicit mention of hypertensive phase.

Similarly, the need for additional medication to control IOP steadily increases in patients with the AGV models, but remains relatively stable with the BGI.[32] Some researchers have suggested that the term hypertensive phase is inappropriate for the AGV, because in most cases the early rise in IOP is not transient but persists and is later reduced only with adjunctive medication.[30]

There is evidence that part of this difference between the AGV and nonvalved implants is due to the timing of the first contact between aqueous humor and the surgical wound. It is generally accepted, that growth factors in the aqueous exert fibrogenic effects on the filtering bleb.[3] Early hypotony with nonvalved implants is avoided by ligating or occluding the devices with a stent to prevent immediate drainage of aqueous. This configuration has the extra advantage of avoiding early contact between aqueous and the conjunctiva of the newly formed bleb, possibly protecting from excessive exposure to TGF-β and other cytokines. Ligation or stenting of the tube delays aqueous flow through the device until wound healing has passed the inflammatory phase and the hydraulic conductivity of the bleb has decreased enough to avoid hypotony.[33] In the AGV, the flow restrictor in the device reduces the incidence of hypotony,[25,34,35] but still permits immediate drainage of some aqueous, which, when exposed to the subtenon fibroblasts, may enhance the degree of bleb encapsulation. Since the final IOP is largely determined by the rate of aqueous resorption from the filtering bleb and the valve mechanism of the AGV is designed to open at pressures of approximately 10 to 12 mm Hg, it should not in principle contribute to failure to control IOP. However, there have been reports of failure due to valves damaged during the implantation procedure.[36,37] In addition, because of the lower incidence of hypotony, the mean final IOP may be slightly higher for AGVs than for nonvalved devices.

Our data suggest that base plate surface topography is also a factor in the clinically observed differences in encapsulation rates. Both AGV models show distinctly rough surfaces with an RMS roughness that is approximately one order of magnitude greater than that of the BGI and MDI (Figs. 4, 6). A possible explanation of the higher rate of hypertensive phase after AGV implantation (both types) is early attachment of tenon fibroblasts to the implant; indeed, in our experimental setup, cells adhered best to the rough surfaces (Fig. 5). Although the differences in macroscopic design and base plate material of the devices used in this study prohibit a valid quantitative comparison, it is evident that there are marked differences in the ability of cells to adhere to the investigated surfaces in vitro. The number of attached cells per area appears to correlate very well with the measured surface roughness in our study ($R^2 = 0.82$, Fig. 7A).

The effects of surface structure on cell adhesion have been extensively studied with other implant designs, materials, and cell types, and there is a clear correlation between surface roughness and cell adhesion.[38–40] Moreover, fibroblast growth is known to be anchorage dependent. Adhesion via integrins greatly enhances growth factor signaling and is a prerequisite for activation, proliferation, and ECM deposition (for a review, see Chiquet et al.[41]). Hence, initial tenon fibroblast adhesion to the implant surface, with subsequent activation and proliferation, could facilitate the formation of thick fibrovascular tissue and be an explanation for the higher incidence of the hypertensive phase and rapid encapsulation of the AGV.

It is worth noting that in our experiments there appeared to be slightly better adhesion of cells on the silicone surfaces when compared with that on the polypropylene devices of similar roughness (i.e., AGV FP7 versus S-2 at 1.5 and 1.3 μm, and BGI

versus MDI at 0.1 and 0.07 μm). This finding may be indicative of topographic influences other than RMS roughness (e.g., homogeneity of texture or sharp versus rounded edges), but could also be the result of surface chemical effects. Our results do not show a strong correlation between collagen adsorption (as surrogate for surface chemistry) and cell adhesion on the investigated surfaces. However, there is a difference in the mean amount of collagen adsorbed between the base plate materials with more collagen immunologically detected on the polypropylene devices (data not shown). This is in accordance with the observation that polypropylene implants produce a more pronounced inflammatory response in a rabbit model than silicone implants.[12] In our in vitro experiments protein adsorption does not appear to contribute much to cell adhesion, whereas roughness seems to exert the predominant effect.

A limitation of our study is the difficulty in transferring our ex vivo results to the clinical setting. It is not clear whether attachment of cells occurs at the early stages of wound healing after implantation. On clinical exploration of encapsulated blebs, the fully formed fibrous capsule is usually not visibly adherent to the implant in situ, and at the time of intervention, the capsules are typically removed without macroscopically visible adherence to the implant.

An alternative explanation of the increased tendency for encapsulation of rough implants may be stretch-mediated activation of fibroblasts through micromovement of the tenon and conjunctiva on top of the surface of the base plate. It has been shown that fibroblasts react to mechanical stress by increasing the expression of actin stress fibers as well as ECM components.[41] Wilcox and Kadri[14,15] presented evidence that this mechanism is active in tenon fibroblasts around the GDD, showing that collagen fibers and cells align along the direction of tension caused by sharp edges or bulky base plates. The RhoA/Rock signaling pathway appears to play a prominent role in this response to mechanical stimuli.[42,43] RhoA/Rock activation has also been shown to be a prerequisite for transdifferentiation of tenon fibroblasts into myofibroblasts,[44] a cell type abundantly found in the thick fibrovascular layer of encapsulated blebs.[45] Thus, micromovements of the bleb on the rough surfaces of the Ahmed base plates may influence fibroblast activity and ECM deposition. On smoother devices, where there is likely to be less friction, one might hypothesize that the tissue could move more freely over the implant surface, with less stretching of fibroblasts and a correspondingly lower incidence of bleb encapsulation.

Whether through early cell adhesion, mechanical stimulation of the cells, or both, the higher surface roughness of some GDD shown in this study is likely to have an impact on bleb fibrosis and failure to control IOP. It may also provide an explanation of why antiproliferative substances like MMC of 5-FU are not as beneficial in GDD as in conventional filtration surgery. Manufacturers should therefore consider specifically designing base plates with smoother surfaces.

In summary, although this semiquantitative study does not permit definitive conclusions regarding the role of GDD surface texture in the subsequent development of bleb encapsulation, it provides some evidence that surface texture is of importance. The influence of surface topography of GDDs on tenon fibroblast attachment and implant encapsulation and the potential benefits of surface modification of implants warrant further investigation.

Acknowledgments

The authors thank Heinz Duschner and Hermann Götz (Institute for Applied Structure and Microanalysis) for providing access to and technical assistance with the confocal laser scanning microscope.

References

1. Gedde SJ, Schiffman JC, Feuer WJ, et al. Treatment outcomes in the tube versus trabeculectomy study after one year of follow-up. *Am J Ophthalmol.* 2007;143(1):9–22.
2. Nguyen QH. Primary surgical management refractory glaucoma: tubes as initial surgery. *Curr Opin Ophthalmol.* 2009;20(2):122–125.
3. Molteno AC, Fucik M, Dempster AG, et al. Otago glaucoma surgery outcome study: factors controlling capsule fibrosis around Molteno implants with histopathological correlation. *Ophthalmology.* 2003;110(11):2198–2206.
4. Hong CH, Arosemena A, Zurakowski D, et al. Glaucoma drainage devices: a systematic literature review and current controversies. *Surv Ophthalmol.* 2005;50(1):48–60.
5. Kurnaz E, Kubaloglu A, Yilmaz Y, et al. The effect of adjunctive mitomycin C in Ahmed glaucoma valve implantation. *Eur J Ophthalmol.* 2005;15(1):27–31.
6. Irak I, Moster MR, Fontanarosa J. Intermediate-term results of Baerveldt tube shunt surgery with mitomycin C use. *Ophthalmic Surg Lasers Imaging.* 2004;35(3):189–196.
7. Autrata R, Helmanova I, Oslejskova H, et al. Glaucoma drainage implants in the treatment of refractory glaucoma in pediatric patients. *Eur J Ophthalmol.* 2007;17(6):928–937.
8. O'Malley Schotthoefer E, Yanovitch TL, Freedman SF. Aqueous drainage device surgery in refractory pediatric glaucomas: I. long-term outcomes. *J AAPOS.* 2008;12(1):33–39.
9. Picht G, Welge-Luessen U, Grehn F, et al. Transforming growth factor beta 2 levels in the aqueous humor in different types of glaucoma and the relation to filtering bleb development. *Graefes Arch Clin Exp Ophthalmol.* 2001;239(3):199–207.
10. Meyer-Ter-Vehn T, Grehn F, Schlunck G. Localization of TGF-beta type II receptor and ED-A fibronectin in normal conjunctiva and failed filtering blebs. *Mol Vis.* 2008;14:136–141.
11. Djodeyre MR, Peralta Calvo J, Abelairas Gomez J. Clinical evaluation and risk factors of time to failure of Ahmed glaucoma valve implant in pediatric patients. *Ophthalmology.* 2001;108(3):614–620.
12. Ayyala RS, Harman LE, Michelini-Norris B, et al. Comparison of different biomaterials for glaucoma drainage devices. *Arch Ophthalmol.* 1999;117(2):233–236.
13. Ayyala RS, Michelini-Norris B, Flores A, et al. Comparison of different biomaterials for glaucoma drainage devices: Part 2. *Arch Ophthalmol.* 2000;118(8):1081–1084.
14. Kadri OA, Wilcox MJ. Surface tension controls capsule thickness and collagen orientation in glaucoma shunt devices. *Biomed Sci Instrum.* 2001;37:257–262.
15. Wilcox M, Kadri OA. Force and geometry determine structure and function of glaucoma filtration capsules. *Ophthalmologica.* 2007;221(4):238–243.
16. Hinkle DM, Zurakowski D, Ayyala RS. A comparison of the polypropylene plate Ahmed glaucoma valve to the silicone plate Ahmed glaucoma flexible valve. *Eur J Ophthalmol.* 2007;17(5):696–701.
17. Ishida K, Netland PA, Costa VP, et al. Comparison of polypropylene and silicone Ahmed glaucoma valves. *Ophthalmology.* 2006;113(8):1320–1326.
18. Minckler DS, Francis BA, Hodapp EA, et al. Aqueous shunts in glaucoma: a report by the American Academy of Ophthalmology. *Ophthalmology.* 2008;115(6):1089–1098.
19. Pakravan M, Homayoon N, Shahin Y, et al. Trabeculectomy with mitomycin C versus Ahmed glaucoma implant with mitomycin C for treatment of pediatric aphakic glaucoma. *J Glaucoma.* 2007;16(7):631–636.
20. Schwartz KS, Lee RK, Gedde SJ. Glaucoma drainage implants: a critical comparison of types. *Curr Opin Ophthalmol.* 2006;17(2):181–189.
21. Cantor LMD, Burgoyne JMD, Sanders SMD, et al. The effect of mitomycin C on Molteno implant surgery: a 1-year randomized, masked, prospective study. *J Glaucoma.* 1998;7(4):240.
22. Heuer DK, Lloyd MA, Abrams DA, et al. Which is better? One or two?—a randomized clinical trial of single-plate versus double-

plate Molteno implantation for glaucomas in aphakia and pseudophakia. *Ophthalmology.* 1992;99(10):1512–1519.

23. Lloyd MA, Baerveldt G, Fellenbaum PS, et al. Intermediate-term results of a randomized clinical trial of the 350- versus the 500-mm^2 Baerveldt implant. *Ophthalmology.* 1994;101(8):1456–1463; discussion 1463–1464.
24. Britt MT, LaBree LD, Lloyd MA, et al. Randomized clinical trial of the 350-mm^2 versus the 500-mm^2 Baerveldt implant: longer term results—is bigger better? *Ophthalmology.* 1999;106(12):2312–2318.
25. Ayyala RS, Zurakowski D, Smith JA, et al. A clinical study of the Ahmed glaucoma valve implant in advanced glaucoma. *Ophthalmology.* 1998;105(10):1968–1976.
26. Ayyala RS, Zurakowski D, Monshizadeh R, et al. Comparison of double-plate Molteno and Ahmed glaucoma valve in patients with advanced uncontrolled glaucoma. *Ophthalmic Surg Lasers.* 2002;33(2):94–101.
27. Stewart WC, Connor AB, Pitts RA. Prognostic factors and postoperative course following single-plate Molteno implantation. *Doc Ophthalmol.* 1994;86(4):409–417.
28. Lloyd MA, Baerveldt G, Nguyen QH, et al. Long-term histologic studies of the Baerveldt implant in a rabbit model. *J Glaucoma.* 1996;5(5):334–339.
29. Susanna R, Latin American Glaucoma Society Investigators. Partial Tenon's capsule resection with adjunctive mitomycin C in Ahmed glaucoma valve implant surgery. *Br J Ophthalmol.* 2003;87(8):994–998.
30. Nouri-Mahdavi K, Caprioli J. Evaluation of the hypertensive phase after insertion of the Ahmed glaucoma valve. *Am J Ophthalmol.* 2003;136(6):1001–1008.
31. Wu SC, Huang SC, Lin KK. Clinical experience with the Ahmed glaucoma valve implant in complicated glaucoma. *Chang Gung Med J.* 2003;26(12):904–910.
32. Tsai JC, Johnson CC, Kammer JA, et al. The Ahmed shunt versus the Baerveldt shunt for refractory glaucoma II: longer-term outcomes from a single surgeon. *Ophthalmology.* 2006;113(6):913–917.
33. Molteno AC, Polkinghorne PJ, Bowbyes JA. The Vicryl tie technique for inserting a draining implant in the treatment of secondary glaucoma. *Aust N Z J Ophthalmol.* 1986;14(4):343–354.
34. Coleman AL, Hill R, Wilson MR, et al. Initial clinical experience with the Ahmed glaucoma valve implant. *Am J Ophthalmol.* 1995;120(1):23–31.
35. Huang MC, Netland PA, Coleman AL, et al. Intermediate-term clinical experience with the Ahmed glaucoma valve implant. *Am J Ophthalmol.* 1999;127(1):27–33.
36. Trigler L, Proia AD, Freedman SF. Fibrovascular ingrowth as a cause of Ahmed glaucoma valve failure in children. *Am J Ophthalmol.* 2006;141(2):388–389.
37. Moss EB, Trope GE. Assessment of closing pressure in silicone Ahmed FP7 glaucoma valves. *J Glaucoma.* 2008;17(6):489–493.
38. Jain R, Von Recum AF. Fibroblast attachment to smooth and microtextured PET and thin cp-ti films. *J Biomed Mater Res A.* 2004 1;68(2):296–304.
39. Mustafa K, Odén A, Wennerberg A, et al. The influence of surface topography of ceramic abutments on the attachment and proliferation of human oral fibroblasts. *Biomaterials.* 2005;26(4):373–381.
40. Meredith DO, Eschbach L, Riehle MO, et al. Microtopography of metal surfaces influence fibroblast growth by modifying cell shape, cytoskeleton, and adhesion. *J Orthop Res.* 2007;25(11):1523–1533.
41. Chiquet M, Gelman L, Lutz R, et al. From mechanotransduction to extracellular matrix gene expression in fibroblasts. *Biochim Biophys Acta.* 2009;1793(5):911–920.
42. Chiquet M, Sarasa-Renedo A, Tunç-Civelek V. Induction of tenascin-c by cyclic tensile strain versus growth factors: distinct contributions by rho/ROCK and MAPK signaling pathways. *Biochim Biophys Acta.* 2004 17;1693(3):193–204.
43. Sarasa-Renedo A, Tunç-Civelek V, Chiquet M. Role of Rhoa/Rock-dependent actin contractility in the induction of tenascin-c by cyclic tensile strain. *Exp Cell Res.* 2006 1;312(8):1361–1370.
44. Meyer-ter-Vehn T, Sieprath S, Katzenberger B, et al. Contractility as a prerequisite for TGF-beta-induced myofibroblast transdifferentiation in human tenon fibroblasts. *Invest Ophthalmol Vis Sci.* 2006;47(11):4895–4904.
45. Classen L, Kivelä T, Tarkkanen A. Histopathologic and immunohistochemical analysis of the filtration bleb after unsuccessful glaucoma seton implantation. *Am J Ophthalmol.* 1996;122(2):205–212.